

Cosmological tests of modified gravity: constraints on $F(R)$ theories from the galaxy clustering ratio

Julien Bel¹, Philippe Brax², Christian Marinoni³ & Patrick Valageas²

¹ *INAF - Osservatorio Astronomico di Brera, Via Brera 28,
20122 Milano, via E. Bianchi 46, 23807 Merate, Italy*

² *Institut de Physique Théorique, CEA, IPhT, F-91191 Gif-sur-Yvette, Cédex, France
CNRS, URA 2306, F-91191 Gif-sur-Yvette, Cédex, France*

³ *Aix Marseille Université, Université de Toulon,
CNRS, CPT UMR 7332, 13288, Marseille, France*

Institut Universitaire de France, 103, bd. Saint-Michel, F-75005 Paris, France

(Dated: June 21, 2018)

The clustering ratio η , a large-scale structure observable originally designed to constrain the shape of the power spectrum of matter density fluctuations, is shown to provide a sensitive probe of the nature of gravity in the cosmological regime. We apply this analysis to $F(R)$ theories of gravity using the luminous red galaxy (LRG) sample extracted from the spectroscopic Sloan Digital Sky Survey (SDSS) data release 7 and 10 catalogues. We find that General Relativity (GR), complemented with a Friedmann-Robertson-Walker (FRW) cosmological model with parameters fixed by the Planck satellite, describes extremely well the clustering of galaxies up to $z \sim 0.6$. On large cosmic scales, the absolute amplitude of deviations from GR, $|f_{R_0}|$, is constrained to be smaller than 4.6×10^{-5} at the 95% confidence level. This bound makes cosmological probes of gravity almost competitive with the sensitivity of Solar System tests, although still one order of magnitude less effective than astrophysical tests. We also extrapolate our results to future large surveys like Euclid and show that the astrophysical bound will certainly remain out of reach for such a class of modified-gravity models that only differ from Λ CDM at low redshifts.

PACS numbers: 98.80.-k

Perplexing observations, such as the accelerated expansion of the universe (the dark energy phenomenon [1, 2]), the rotation curves of galaxies or the gravitational lensing from large clusters of galaxies (the dark matter phenomenon [3, 4]), seem to point towards new phenomena beyond the physics already tested in the laboratory or in the Solar System. In particular, they may be associated with departures from Einstein's theory of gravity [5, 19].

Powerful tests on Solar System [6] and astrophysical [7, 8] scales, however, seem to confirm GR predictions and impose stringent limits on modified gravity theories. As a consequence, realistic alternative theories should incorporate non-linear mechanisms that ensure convergence to General Relativity on small scales and high-density environments. In particular, the fifth force which emerges as a generic prediction of modified gravity models, obtained by adding a single scalar degree of freedom φ to Einstein's equations, can be effectively *screened* either by the Vainshtein [9], the Damour-Polyakov [10], or the chameleon [11–13] mechanisms. Models with the chameleon property converge to GR on cosmological scales too. As a consequence, intermediate, mildly non-linear scales ($\sim 10h^{-1}\text{Mpc}$) appear as a unique window of opportunity for detecting possible deviations from GR in a large class of models.

Modified gravity models must, in a first approximation, reproduce the smooth background expansion history of the standard model of cosmology, the Λ -Cold Dark Matter (Λ CDM) paradigm. To distinguish and falsify various competing gravitational proposals it is thus necessary to analyze characteristic observables of

the perturbed sector of the model. Indeed, to lowest order in cosmological perturbations, non-standard gravitational scenarios effectively result in a time- and scale-dependent modification of Newton's constant, that is, in a distortion of the dynamical and the statistical properties of characteristic clustering quantities such as the power spectrum [14, 16, 17] and the growing mode $D_+(k, z)$ [and its logarithmic derivative, the growth rate $f(k, z) = \partial \ln D_+ / \partial \ln a$] of linear matter perturbations [18, 19].

Gravity tests on cosmological scales are still far from reaching the precision achieved with small-scales experiments. Several observational shortcomings affect standard probes such as, for example, cosmic shear in weak lensing maps [20, 21], redshift-space distortions [22, 23], and galaxy clustering [14, 16, 17, 24, 25]. Their main observable, the growth rate of dark matter f , for example, cannot be estimated from data without picking a particular model, or at least a parameterization, for gravity [26, 27]. Moreover, although the most generic extensions of GR predict a scale dependent growth rate f , devising a method able to measure $f(k, z)$ at different scales is a formidable observational task [28, 29]. Additionally, in all the analyses it is assumed that the bias is the same for both modified and standard gravity models. This is a non-trivial ansatz, since not only the growth of structures is expected to be different in modified theories of gravity, but the gravitational potential, which plays a key role in the formation of galaxies, and hence in determining their biasing properties, changes. Finally, most of these probes rely on a precise and challenging measurement of

the mean galaxy density on large cosmic scales [30].

Here we show how to address most of these issues via a new gravitational probe, the clustering ratio η [31] (hereafter BM14), [32]. Due to its peculiar definition, this cosmological observable naturally accounts for possible scale-dependent growth rates of matter fluctuations. In particular, on linear scales the η amplitude is constant as a function of time in general smooth dark energy (w -CDM) models but acquires a characteristic time dependence for modified gravity models. Observational information are inferred from the analysis of the luminous red galaxy (LRG) sample extracted from the SDSS data release 7 [47] as well as from the data release 10 [48].

In section I, we define the clustering ratio and relate its measurement to the real-space matter density power spectrum in the quasi-linear regime. In section II, we introduce the models of modified gravity that we shall be using in this paper, i.e. $F(R)$ theories in the large curvature regime. These models serve as a first illustration of our results using the clustering ratio. The same methods can be applied to more complex models, a study which is left for future work. We also extract the clustering ratio and its redshift dependence from the SDSS catalogue. In section III, we consider the different systematic effects which hamper the accuracy of the clustering ratio comparison with data. This section can be skipped by the reader who is only interested in the applications to modified gravity. Finally in section IV, we obtain constraints on $F(R)$ models when either keeping the matter fraction Ω_{m0} fixed or relaxing it using the Planck prior. We conclude in section V.

I. THE GALAXY CLUSTERING RATIO AS A GRAVITATIONAL PROBE

A. Several clustering ratios and their relations

The galaxy clustering ratio in redshift space,

$$\eta_g^s(r, x; z) \equiv \frac{\xi_{g,x}^s(r)}{(\sigma_{g,x}^s)^2} \quad (1)$$

$$= \frac{\int_0^\infty dk k^2 \int_{-1}^1 d\mu P_g^s(k, \mu; z) W(kx)^2 \frac{\sin(kr)}{kr}}{\int_0^\infty dk k^2 \int_{-1}^1 d\mu P_g^s(k, \mu; z) W(kx)^2}, \quad (2)$$

is defined as the ratio of the correlation function to the variance of the redshift-space galaxy over-density field $\delta_{g,x}^s$, smoothed on a scale x via the filter W , where $W(y) = 3[\sin(y) - y \cos(y)]/y^3$ is the Fourier transform of the unit top-hat, the specific filtering scheme adopted by BM14 to smooth data. Note that the index g labels quantities that are evaluated using galaxies as opposed to matter, and that the superscript s indicates when physical quantities are evaluated in redshift space as opposed to real space. Furthermore, to simplify the analysis, we consider

$$\eta_g^s(n, x; z) \equiv \eta_g^s(r = nx, x; z) \quad (3)$$

as a function of the smoothing scale x for a fixed ratio n between the correlation (r) and the smoothing (x) scales.

At first glance, this second order statistic only provides information about the monopole $P_{g(0)}^s$ of the redshift-space power spectrum of the galaxies. A key result of BM14, however, was to show that on quasilinear scales this second order statistics provides information on a more fundamental and simpler physical quantity, that is, the power spectrum of matter fluctuations in real space $P_g(k, z)$. Indeed

$$\eta_g^s(n, x; z) \approx \eta_g(n, x; z) \approx \eta(n, x; z), \quad (4)$$

where $\eta(n, x; z)$ is the mass clustering ratio in real space,

$$\eta(n, x; z) \equiv \frac{\int_0^\infty dk k^2 P(k, z) W(kx)^2 \frac{\sin(knx)}{knx}}{\int_0^\infty dk k^2 P(k, z) W(kx)^2}. \quad (5)$$

The first approximation in Eq.(4) means that, under some very generic conditions, the amplitude of the galaxy clustering ratio is the same in both real and redshift spaces. In the Λ CDM cosmology, this is exact at the linear level because the linear growing mode $D_+(z)$, and its derivative $f(z) = \partial \ln D_+ / \partial \ln a$, do not depend on scale. This is no longer true in modified gravity theories, which give rise to new scale dependences. In addition, small-scale virial motions, which give rise to the fingers-of-god effect, also contribute to the redshift-space power spectrum and to the clustering ratio. We shall discuss both effects in Sec. III A and show that they do not impact the clustering ratio beyond the percent level.

The second approximation in Eq.(4) means that the amplitude of the galaxy clustering ratio is approximately identical to the amplitude of the analogous statistics for matter fluctuations. This actually involves two properties, that the corrections due to nonlinearities of the biasing scheme can be neglected, and that the scale dependence of bias coefficients does not sufficiently distort the shape of the power spectrum on the relevant scales to significantly modify the clustering ratio η . Both effects will be addressed in turns in Sec. III B and III C.

B. Expected accuracy and applicability

The η formalism was engineered to ease the comparison between data and theoretical predictions. From the observational perspective, the advantage of the galaxy clustering ratio rests on the simplicity and accuracy with which it can be extracted from redshift galaxy catalogs. Indeed, it provides information on $P(k, z)$ without the need of reconstructing the galaxy power spectrum in Fourier space, nor the correlation function of galaxies, along with their covariance matrices; one-point statistics such as counts in cells is all that is needed for its measurement. On the theoretical side, a distinctive feature of the η -statistic is the neat prediction of its amplitude which is virtually independent from any modelling assumption.

On large scales x and r , where $P(k, z)$ is fairly described by a linear approximation, and assuming standard gravity, *i.e.* that the linear growing mode $D_+(z)$ does not depend on scale, the amplitude of η is not only independent from biasing and redshift-space distortion models, but also from linear growth rate of structures, cosmic time, and normalisation of the matter power spectrum. In other terms, there is no need to model and subsequently marginalise over these quantities, a procedure that is known to degrade both the accuracy and the precision of cosmological probes.

Our approach follows from the observation, developed in this paper, that at least one of these characteristic predictions breaks down if modified gravity is responsible for the large scale distribution of matter. Specifically, if a scale dependent growing mode $D_+(k, z)$ is considered, η is not a universal number anymore (at fixed scale x), but becomes a function of cosmic time, as the time dependence no longer factors out in Eq.(5). Clearly, this time dependent signal is also expected in the Λ CDM cosmology if η is estimated on scales where the linear approximation for the power spectrum breaks down. To this purpose, note that the highest precision on η ($\sim 5\%$ from current redshift surveys of galaxies) can be achieved only on scales that are mildly non-linear. For example, on the scale $x = 16h^{-1}\text{Mpc}$ used in this paper, the relative inaccuracy induced on η by adopting a linear power spectrum instead of a non-linear one in Eq.(5) is of order 6% for $n = 2$ and 3% for $n = 3$, as found in FIG. 7 below. Because of this reason, in the rest of this paper we will adopt a non-linear prescription for modeling the matter power spectrum.

What is also crucial for our discussion, is that the estimation of a characteristic observable of the perturbation sector, such as the clustering ratio η , only requires the knowledge of the expansion rate of the universe, *i.e.* prior information about the smooth sector of the theory only. In other words, the measurement of η does not presuppose the premise to be tested, *i.e.* the knowledge of a specific gravitational theory. A prescription for converting redshifts into distances is the only ingredient needed for estimating η from redshift surveys data. Since a large class of interesting modified gravity models predict distance-redshift relations which are indistinguishable from that of the Λ CDM models, the η observable is such that we do not need to re-estimate it in each of the distinct gravitational scenarios we are testing. From this remark follows the central argument of this paper: instead of assuming a gravitational model and using η to fix the expansion rate of the universe in that model, as done by BM14, we here assume the expansion rate known from independent observations (specifically the Planck results [40]) and use η to distinguish different gravitational models, specifically theories where the Einstein-Hilbert action is supplemented by a general function $F(R)$ of the Ricci scalar.

For this testing strategy being effective, the amplitude of the redshift-space galaxy clustering ratio η_g^s , the quan-

tity that can be directly extracted from galaxy surveys, should be predicted from the real space matter power spectrum only (cfr. eq. 4) with an accuracy of $\sim 2\%$. This level of accuracy is indeed enough to place interesting constraints on possible deviations from the standard Λ CDM scenario, notably on the family of $F(R)$ theories investigated in this paper. That this precision is indeed achievable in the spatial and temporal regimes to which current data give access, is discussed in more details in Sec. III.

II. THE CLUSTERING RATIO AND SCREENED $F(R)$ GRAVITY

A. $F(R)$ gravity

As a template for the $F(R)$ gravity models, we choose the bi-parametric form [44–46]

$$F(R) = -2\Lambda c^2 - \frac{f_{R_0} c^2}{N} \frac{R_0^{N+1}}{R^N}, \quad (6)$$

where $f_{R_0} < 0$ is a normalization factor and $N > 0$. This Lagrangian corresponds to the large-curvature regime of the model proposed in [46], which is consistent with Solar-System and Milky-Way constraints thanks to the chameleon mechanism, for $|f_{R_0}| \lesssim 7 \times 10^{-7}$. In the following we will specialize our analysis to the cases $N = 1$ and 2. The background dynamics agree with the reference Λ CDM scenario with the same cosmological parameters. The growth rate of density fluctuations, however, is slightly modified. At the linear level, this follows from the fact that the Newtonian potential Ψ_N , or Newton's constant, are effectively multiplied, in Fourier space, by a scale dependent factor $1 + \epsilon(k, z)$, where

$$\epsilon(k, z) = \frac{k^2}{3(a^2 m^2 + k^2)}, \quad (7)$$

and

$$m^{-2} = 3 \frac{d^2 F}{dR^2} = -3(N+1)f_{R_0} \frac{c^2 R_0^{N+1}}{R^{N+2}}. \quad (8)$$

On large scales, $k \ll am$, GR is recovered, whereas on small scales, within this linear approximation, Newton's constant is larger by a factor 4/3. Stronger gravity implies that structure formation is favored and ultimately results in a matter power spectrum amplitude which is larger than that characterizing the Λ CDM model on mildly non-linear scales, $k \sim 1h\text{Mpc}^{-1}$. For smaller scales and high densities, non-linear effects are no longer negligible and the chameleon mechanism ensures convergence to GR. As $|f_{R_0}|$ goes to zero, m^2 goes to infinity and General Relativity is recovered, hence the Λ CDM scenario, on all cosmological scales. Hereafter, we consider as *reference* Λ CDM, the spatially-flat six-parameter model shown in column 1 (*Best fit*) of Table 2 by [40].

The amplitude of the clustering ratio expected in $F(R)$ gravity is computed using the formalism described in [16]. This combines one-loop perturbation theory [that includes non-linear effects beyond the $\epsilon(k, z)$ factor, such as new quadratic and cubic vertices in the Euler equation generated by the $F(R)$ theory] and a halo model [which takes into account the non-linear impact of the $F(R)$ theory on the halo mass function through the analysis of the modified spherical collapse]. This approach provides a realistic estimate of the real-space matter density power spectrum, from large scales to small scales, that is automatically consistent with one-loop perturbation theory and agrees with numerical simulations up to their highest available wave number, $k \lesssim 3h\text{Mpc}^{-1}$ at $z = 0$ [16].

B. The clustering ratio from SDSS data

We estimate the clustering ratio of the luminous red galaxy (LRG) sample extracted from the SDSS data release 7 [47] as well as from the data release 10 [48]. The first catalogue ($s1$) covers the redshift interval $0.15 < z < 0.43$, has a contiguous sky area of $120 \times 45 \text{ deg}^2$, and comprises 62,652 LRG. The second sample ($s2$), extracted from the SDSS DR10 after removing all the objects in common with $s1$, extends over a deeper interval $0.3 < z < 0.67$ but shallower (and not contiguous) field of view $\sim 3000 \text{ deg}^2$.

The galaxy clustering ratio is estimated, assuming the redshift-distance conversion of the reference ΛCDM model (flat universe with $\Omega_{m0} = 0.3175$), as detailed in [32]. Error bars are derived from a 30 block-jackknife re-sampling of the $s1$ ($s2$) data, excluding, each time, a sky area of $12 \times 14 \text{ deg}^2$ ($10 \times 10 \text{ deg}^2$). This specific scheme to estimate uncertainties when η is estimated from SDSS data was shown to give error bars in excellent agreement ($\sim 8\%$ relative difference) with those deduced from the analysis of the standard deviation displayed by 40 SDSS-like simulations (the LasDamas simulations [49]), which include, by definition, the contribution from cosmic variance. This is suggestive of the fact that η , being defined as a ratio of equal order statistics, and thus containing the same stochastic source, is weakly sensitive to this systematic effect.

Results for scales $9 \leq x \leq 25h^{-1}\text{Mpc}$ and correlation indices $n = 2, 3, 4$ are shown in FIG. 1. Note that the lower limit on x ensures that quasilinear perturbation theory, the framework in which the η formalism is developed, consistently applies, while the upper limit on n is set because measurements are progressively noisier when the correlation length $r = nx$ increases. The scale $x = 16h^{-1}\text{Mpc}$ provides an optimal trade-off that guarantees both theoretical and observational accuracy, and in the following we will only consider the clustering ratio signal extracted on this scale. Additional arguments that justifies the choice of this filtering window will be provided in the next section, where the overall systematic uncertainty affecting our analysis is presented and

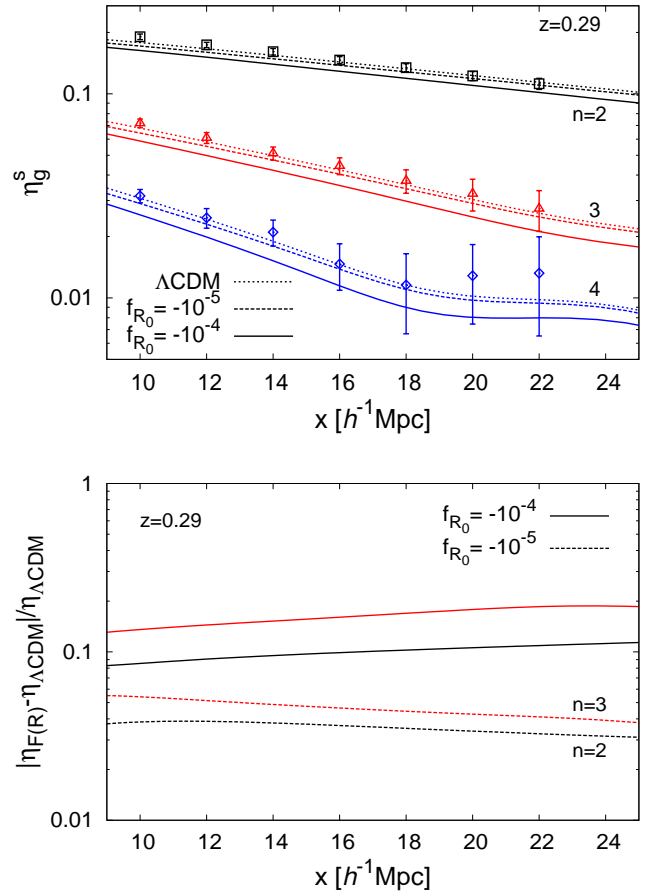


FIG. 1: *Upper panel:* clustering ratio $\eta_g^s(n, x)$ as a function of the filtering scale x for $n = 2$ (squares), $n = 3$ (triangles), and $n = 4$ (diamonds), at $z = 0.29$, the mean redshift of the $s1$ sample. The upper (dotted) line represents the scaling predicted in the reference ΛCDM model (flat model with $\Omega_{m0} = 0.3175$) while the middle (dashed) and lower (solid) lines correspond to the $F(R)$ models with exponent $N = 1$ and normalisation parameters $f_{R0} = -10^{-5}$ and $f_{R0} = -10^{-4}$ respectively. *Lower panel:* relative deviation of the $F(R)$ models from the ΛCDM prediction.

discussed.

A generic yet distinctive feature of the matter power spectrum in $F(R)$ theories is an excess of power on weakly non-linear scales, $0.1 \lesssim k \lesssim 10h\text{Mpc}^{-1}$, with respect to the ΛCDM case. On the scales considered here, $x > 10h^{-1}\text{Mpc}$, we thus expect these theories to predict a smaller clustering ratio $\eta(n, x)$. Indeed, η provides a measure of the ratio of the power spectrum at the characteristic scales $r = nx$ and x , that is, on large scales, its amplitude is roughly given by

$$\eta(n, x) \sim \frac{D_+^2(1/nx, z) \Delta_{L0}^2(1/nx)}{D_+^2(1/x, z) \Delta_{L0}^2(1/x)}, \quad (9)$$

where $\Delta_{L0}^2(k) = k^3 P_{L0}(k)/2\pi^2$ is the initial linear power

per logarithmic interval of k and $D_+(k, z)$ the linear growing mode. The power suppression is effectively what is found in FIG. 1, which illustrates the scale dependence of η in both the reference Λ CDM and $F(R)$ scenarios. Note that the relative deviation between $F(R)$ and Λ CDM predictions is approximately constant, at least over the range of scales displayed, while its amplitude grows with the correlation index n . The uncertainty in the data, however, grows even faster, that is the signal-to-noise ratio decreases as a function of n thereby reducing the discriminatory power of the diagnostic at high n .

In FIG. 2 the amplitude of the clustering ratio estimated at the three different redshifts $z = 0.29, 0.42$, and 0.60 is shown (for the typical quasi-linear scale $x = 16h^{-1}\text{Mpc}$). The clustering ratio signal of the $s1 + s2$ samples on the filtering and correlation scales $x = 16h^{-1}\text{Mpc}$ and $n = 2$ is recovered with a relative inaccuracy of $\sim 3\%$. This figure is indicative of the current performances of the η test as a gravity probe. To better appreciate it, one can contrast this figure with the expected distortions in the clustering ratio signal induced by a non standard growth of cosmic structures. This is done in the lower panels of FIG. 1 and 2, where we show the relative difference (and the redshift scaling) between the amplitude of $\eta(n = 2, x = 16h^{-1}\text{Mpc}, z = 0.29)$ in the Λ CDM and $F(R)$ models. For instance, the η amplitude at $z = 0.29$ in models with $f_{R_0} = -10^{-4}(-10^{-5})$ is nearly $10\%(4\%)$ smaller than predicted by Λ CDM [65]. This is greater than the 2% accuracy of our approximation (4), see Sec. I, which shows that within our framework we can constrain these $F(R)$ models down to $|f_{R_0}| \sim 10^{-5}$.

The sensitivity of the clustering ratio as a probe of the cosmological scenario is further enhanced by the fact that not only the amplitude of the signal is of relevance, but also its different scaling as a function of redshift. Indeed, while in a Λ CDM cosmology the amplitude of η is expected to be almost constant in time, in modified-gravity scenarios, such as $F(R)$ theories, the scale dependence of the effective Newton's constant eventually results in a substantial redshift dependence of the predictions for the amplitude of η . In particular the discrepancy between the $F(R)$ and the Λ CDM predictions amplifies with time as they are indistinguishable at early cosmic epochs (see bottom panel of FIG. 2). A detection of a statistically significant redshift dependence of the $\eta(n, x; z)$ signal is therefore a strong and unequivocal signature of deviations from the Λ CDM scenario. Thus, in the Λ CDM case, from $z = 1$ to $z = 0$ the clustering ratio at $x = 16h^{-1}\text{Mpc}$ decreases by 3.7% , because of the nonlinear growth of the power spectrum (which of course gives rise to a scale dependence as it introduces the nonlinear scale of matter clustering). For $f_{R_0} = -10^{-4}(-10^{-5})$, it decreases by $8.4\%(7.1\%)$. This greater decrease at low redshift than for the Λ CDM case is due to the additional scale dependence associated with modified gravity, which now appears at both the linear and nonlinear levels.

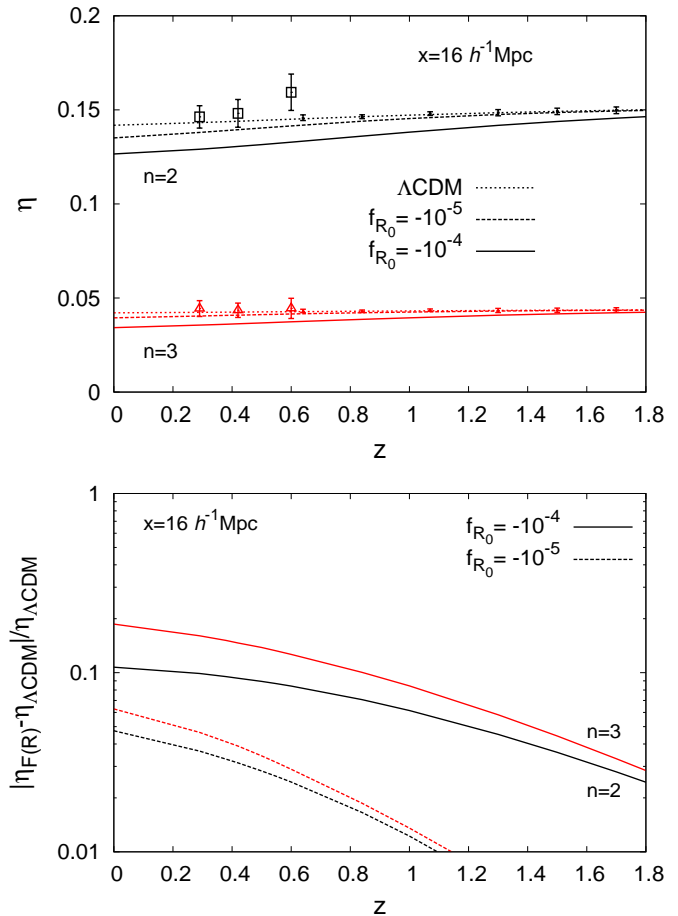


FIG. 2: *Upper panel:* clustering ratio $\eta_g^s(n, x, z)$ measured in three different redshift intervals centered at $z = 0.29$ ($s1$ sample), 0.42 and 0.60 ($s2$ sample). The redshift intervals in which the $s2$ sample is split are defined so that error bars are roughly equivalent to that estimated from the $s1$ sample. We show measurements obtained for the smoothing scale $x = 16h^{-1}\text{Mpc}$ and for the correlation indices $n = 2$ (squares) and $n = 3$ (triangles). We also show the amplitude of the clustering ratio predicted by the reference Λ CDM scenario (upper dotted lines) and by the $F(R)$ models with exponent $N=1$ and with normalization parameters $f_{R_0} = -10^{-5}$ (middle dashed lines) and $f_{R_0} = -10^{-4}$ (lower solid lines). We give an example typical of future surveys: the small black error bars on the standard Λ CDM curve (dotted) show forecasts for measurements in bins of size $\Delta z \sim 0.2$ from an $15,000 \text{ sq. deg.}$ survey of 7×10^6 galaxies, which closely matches what is expected from the Euclid mission [43]. *Lower panel:* relative deviation of the $F(R)$ models from the Λ CDM prediction.

III. SYSTEMATICS

The next step is to make sure that residual systematic effects do not compromise the effectiveness of the η formalism in disentangling $F(R)$ models from the reference Λ CDM. The accuracy of the relation $\eta_g^s = \eta_g$ was tested using various numerical simulations of the large

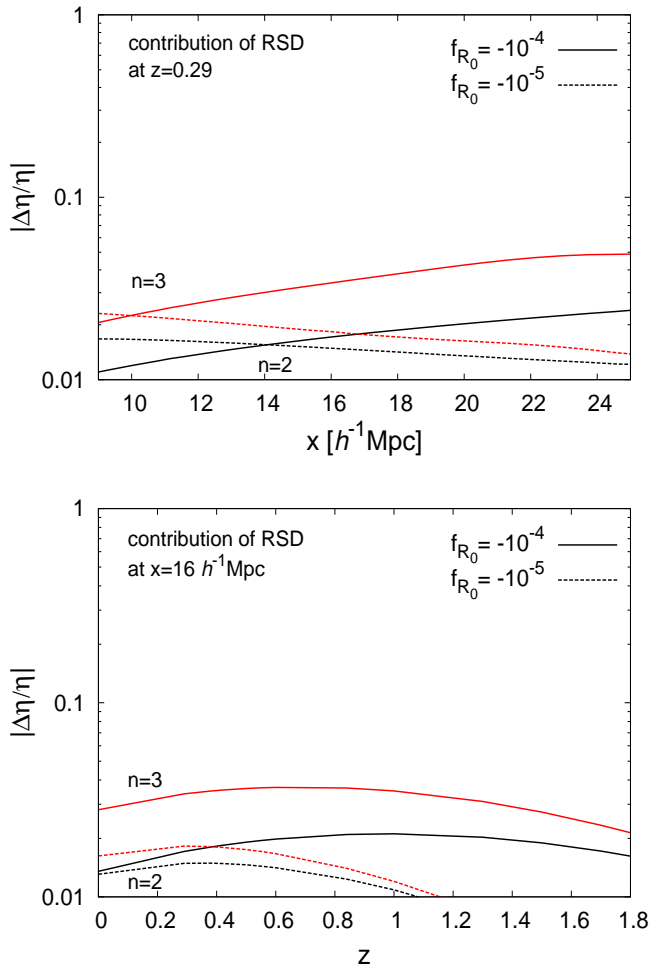


FIG. 3: Impact of linear redshift-space distortions on the amplitude of the clustering ratio, as a function of scale (*upper panel*) and redshift (*lower panel*). We show the relative deviation between η_g and η_g^s [computed using the model in Eq.(10)].

scale structure of the universe in a Λ CDM model by [31, 32]. In particular, under blind test conditions, the η formalism was shown to recover, in an unbiased way, the value of the cosmological parameters used in the simulations. Here, our purpose is to explore whether the chain of approximations shown in Eq.(4) holds to percentage level precision also in the context of the $F(R)$ model of Eq.(6). We also consider the impact of nonlinearities and baryonic effects on the matter power spectrum itself.

A. Redshift-space distortions.

The first approximation in Eq.(4) is the use of the real-space clustering ratio to estimate the observed redshift-space galaxy clustering ratio. Therefore, in this section we estimate the impact of redshift space distortions (RSD). In the Λ CDM cosmology, an interesting feature

of the clustering ratio is that in the linear limit it is insensitive to redshift space distortions, $\eta_g^s = \eta_g$. This is because the linear Kaiser effect [39] only multiplies the power spectrum by a factor $(1 + \beta\mu^2)^2$ in redshift space, as in Eq.(10) below, and this scale-independent factor cancels out in the ratio (2). This simplicity is lost when we consider quasi-linear scales (where non-linear motions are expected to contaminate the cosmological signal) or exotic models of gravity [where RSD might not factor out exactly in Eq.(2)]. This is the case in $F(R)$ scenarios, where the growth rate $f(k, z)$ of linear matter fluctuations depends on the wave number k . As a consequence, a systematic bias results from neglecting the contribution of the RSD to the amplitude of the clustering ratio. We evaluate quantitatively the amplitude of this bias by adopting the Kaiser model, where we write the redshift-space power spectrum of galaxies [cf. Eq.(2)] as

$$P_g^s(k, \mu) = b_1^2 (1 + \beta\mu^2)^2 P(k), \quad \beta(k, z) = \frac{f(k, z)}{b_1}, \quad (10)$$

where b_1 is the linear galaxy bias in redshift space (although the matter real-space power spectrum $P(k)$ includes non-linear corrections as explained in Sec. III D). In the following we take $b_1 = 2$, a value well representing the bias of luminous red galaxies [38]. The relative error that results from neglecting the linear RSD effect is shown in FIG. 3. As expected, the RSD correction is typically of order of the percent and smaller than that arising from neglecting to correct the power spectrum for non-linear effects, see Sec. III D below. It is also smaller than the deviation between the Λ CDM and $F(R)$ real-space predictions for η , as the k -dependent growth rate $f(k, z)$ is damped by the cosine μ and the bias b_1 . Note that this error depends on the parameter f_{R0} and vanishes for $|f_{R0}| \rightarrow 0$ as we converge to the Λ CDM cosmology. In particular, for $x = 16h^{-1}\text{Mpc}$, $z = 0.29$ and $n = 2$, the relative contribution of the redshift-space distortions to the clustering signal is 1.5%/(1.4%) for $f_{R0} = -10^{-4}$ /(-10^{-5}).

In addition to the corrections associated with large-scale coherent flows discussed above, small-scale random motions of galaxies within virialized structures also contribute to the redshift-space power spectrum, giving rise to the fingers-of-god effect. The leading order contribution of these small-scale effects to the amplitude of η can be estimated by using Eq.(9) of [32]. This model assumes that a Gaussian kernel fairly describes the distribution of pairwise velocities along the line of sight, with a dispersion $\sigma_{12} = 300\text{km/s}$. The amplitude of the relative error induced by neglecting contributions from non-linear peculiar velocities is shown in FIG. 4. As expected, the systematic error decreases rapidly with the filtering scale x (given the incoherent nature of small-scale non-linear motions), and appears to be almost insensitive to cosmic time (since motions induced by local gravity are detached from the Hubble expansion). More importantly, on the scale relevant to our analysis ($x = 16h^{-1}\text{Mpc}$) the error is of order $\sim 2\%$ and comparable to the very same preci-

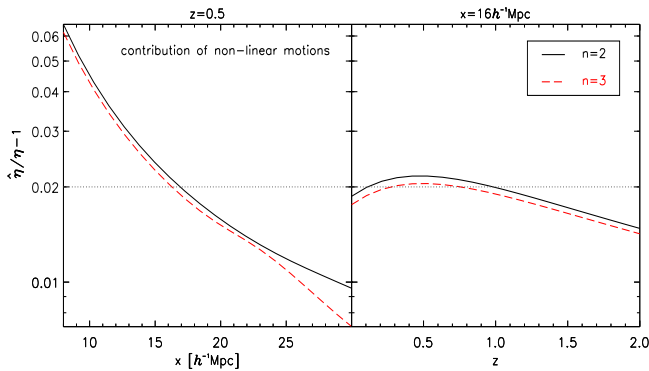


FIG. 4: Impact of non-linear random motions on the amplitude of the clustering ratio, as a function of scale (*left panel*) and redshift (*right panel*). We show the relative deviation between the η amplitude predicted before and after correcting the clustering ratio estimates with a Gaussian model of the galaxy velocity dispersion [cf. Eq.(9) of [32]].

sion ($\sim 1.6\%$) with which phenomenological prescriptions available in the literature are effective in modelling these random motions (at least those simulated via numerical experiments) [32]. Because we consider modified gravity models that are very close to the Λ CDM cosmology, we can expect these small-scale effects to keep the same order of magnitude.

Thus, the corrections to the clustering ratio due to large-scale coherent flows (more specifically, their scale dependence generated by modified gravity) and to small-scale motions are of the same order of magnitude. Interestingly however, while the large-scale RSD tends to suppress the amplitude of the clustering ratio on a given scale x , the non-linear random motions act in the opposite direction. The global resulting inaccuracy in the relation $\eta_g^s = \eta_g$ is thus expected to be smaller than 1%. We emphasize that this figure is much smaller than the precision with which the large-scale evolution of velocity fields is described by linear theory [41]. Note, also, that these values are significantly smaller than the relative difference between the amplitude of η predicted in $F(R)$ models (with parameters $f_{R_0} = -10^{-4}$ or $f_{R_0} = -10^{-5}$) and the Λ CDM value. Therefore, the residual effects induced by the choice of not modelling redshift-space distortions do not impair the ability of the clustering ratio to constrain f_{R_0} down to $|f_{R_0}| \simeq 10^{-5}$.

B. Non-linear bias

After redshift-space distortions, the second approximation in Eq.(4) is to neglect corrections due to galaxy biasing. We first investigate in this section the accuracy of the statement that the clustering ratio amplitude is independent from the galaxy biasing function and its possible nonlinear character. As described in Refs.[31, 33],

this result holds on those scales x where a local deterministic biasing scheme, $\delta_{g,x} = \sum_i b_{i,x} \delta_x^i / i!$, fairly describes the relation between galaxy and matter density fields and the constraints $|b_{1,x}/b_{2,x}| > \sigma_x^2$ and $1 > |b_{2,x}\xi(r)|$ on the lower order biasing coefficients are both satisfied. For example, on the scale $x = 16h^{-1}\text{Mpc}$, the inaccuracy in the second approximation shown in Eq.(4) is $0.8(/0.6)\%$ for $n = 2(/3)$ at $z = 0.5$, and $0.8(/0.3)\%$ at $z = 0(/1)$ for $n = 2$. These figures are computed by evaluating the contribution of higher-order, bias dependent corrections, using Eq.(42) of [33], under the assumption of a non-linear galaxy biasing scheme with $b_{1,x} = 2$ and $b_{2,x} = -0.2$, fairly representative of what is found from the analysis of red galaxy samples similar to those used in this paper [36–38].

As a comparison, if, as usually done in the literature, one neglects higher order biasing contributions to the relation between the *rms* of galaxy and matter fluctuations, the precision of the approximated relation $\sigma_{g,x} \approx b_{1,x}\sigma_x$ (on the same scale x discussed above) is roughly 5 times poorer, being affected by a relative systematic error of nearly 4%.

As we consider screened $F(R)$ models that are very close to the Λ CDM cosmology, we expect the galaxy biasing mechanisms to be essentially the same as in the standard cosmological scenario. Thus, the impact of non-linear biasing corrections should remain about 1% or less. This is significantly smaller than the expected signal distortions induced by non-standard gravity with $|f_{R_0}| \gtrsim 10^{-5}$, see FIG. 2, and below the accuracy of 2% that we aim at in this paper. Therefore, we can neglect these nonlinear biasing corrections for our purposes. This also simplifies the analysis as it avoids resorting to a more refined, bias-dependent, theoretical prediction for the η amplitude.

C. Scale-dependent bias

We have seen in the previous section that nonlinear biasing does not give rise to significant corrections on the large scales that we consider in this paper. However, even within a linear bias model, another source of systematics due to the bias arises from the scale dependence of the galaxy bias, which can distort the shape of the correlation function and mimic the scale-dependent growth associated with a modified-gravity scenario.

1. Sensitivity to scale-dependent biasing

Since the clustering ratio is engineered to extract cosmological information encoded in the galaxy distribution on a given filtering scale x , this statistics is by construction independent from any possible (real-space) scale dependence $b(x)$ of the biasing function on smaller scales. Thus, the η formalism is built upon the hypothesis that biasing is local, i.e. by explicitly neglect-

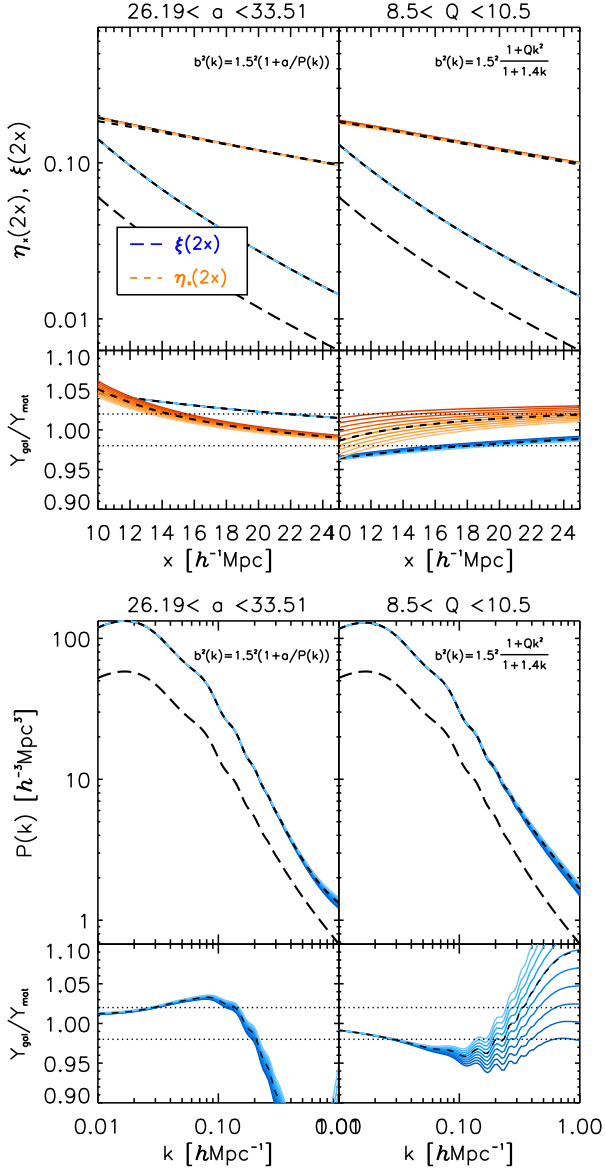


FIG. 5: Impact of scale-dependent contributions of the biasing models, here the P- and Q-models, on the ratio between galactic and matter quantities Y where Y can be either the power spectrum $P(k)$, the 2-point correlation $\xi(x)$ or the clustering ratio $\eta(2, x)$. The characteristic parameters of the biasing models (a and Q) are varied within their 95% confidence interval determined by [51]. In all cases, the η dependence on bias is less than two percent.

ing the possibility that galaxy and matter power spectra are related by scale dependent operators in Fourier-space [$P_g(k) = b^2(k)P(k)$] on larger scales r beyond the filtering scale x . However, some degree of biasing depending on the wave number k is naturally expected on cosmological scales. Fortunately, it is unlikely that neglecting this effect on large scales r induces an appreciable systematic error in the predicted amplitude of η_g . Indeed, tests performed on LasDamas numerical simulations of the large scale structure of the universe also confirmed, indepen-

dently, that possible systematic effects induced by a non local, k -dependent galaxy bias can be safely neglected on the scales explored in our analysis [32].

This is well illustrated by the following example in which we consider the Q-model $b^2(k) = b_1^2(1 + Qk^2)/(1 + Ak)P_L(k)/P(k)$ [50] with parameters $A = 1.4$ and $Q = 9.6$ [51]. The relative variation of the squared bias, $\Delta b^2/b^2$, is as high as 8% in the interval $0.01 < k < 1h/\text{Mpc}$, but results in η changing by only $\sim 0.8\%$ on the relevant scales $x = 16h^{-1}\text{Mpc}$ and $r = 2x$.

This substantial independence of the clustering ratio on scale-dependent biasing is also illustrated in FIG. 5, where the ratios Y_g/Y_{matter} are represented for both the Q-model and the P-model, defined by $b^2(k) = (b_1^2 P_L(k) + a)/P(k)$, which, according to [52], has a more solid grounding in physics than the Q-model (the parameter a corresponds to a shot-noise contribution that can arise if galaxies Poisson sample the matter density field). The quantities Y are either the power spectrum, the correlation function ξ or the clustering ratio η . In each case, the quantity Y_{matter} is multiplied by a constant bias $b_1 = 1.5$, which actually cancels out in the case of η . The width of the curves shows the impact of the variation of the bias parameters a and Q within their 2σ confidence range [51]. As can be seen in the figure, the scale dependence of the bias predicted by these models does not modify η_g by more than two percents, at $x = 16h^{-1}\text{Mpc}$, whereas it has a significantly greater effect on the power spectrum and the correlation function. Moreover, varying the parameters of these bias models within 2σ intervals does not further modify η beyond 2%. This is particularly important for the applications to modified gravity, as the knowledge of the biasing function and the range of the biasing parameters could be affected as compared with the Λ -CDM cosmology. These results show that the dependence of the clustering ratio on the scale dependence of the bias, through both the biasing parameters and the functional form of the biasing model, is within the required accuracy in order to derive sensible bounds on modified gravity.

2. Comparison with marginalizing analysis based on the power spectrum

A more traditional approach, especially when one uses the power spectrum itself as a probe of cosmology rather than the clustering ratio, is to marginalize over the nuisance parameters of the biasing model. Within a specific bias model, this allows one to take into account the possible change of the bias parameters associated with $F(R)$ scenarios. This approach, however, overlooks the possibility that the shape of the biasing function in $F(R)$ scenarios might be poorly described by the reference biasing model, and therefore that systematic errors might be introduced when marginalising over an improper function.

To substantiate this argument, we simulate the matter

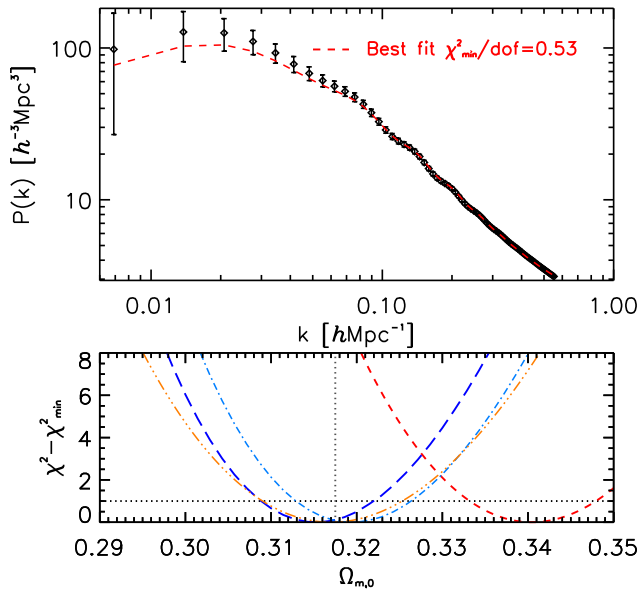


FIG. 6: *Upper panel:* galaxy power spectrum (diamonds) simulated using the *reference* Λ CDM model ($\Omega_{m0} = 0.3175$) and the Q-model for describing scale-dependent galaxy biasing ($b_1 = 1.5$, $Q = 9.6h^{-2}\text{Mpc}^2$ and $A = 1.4h^{-1}\text{Mpc}$). Error bars roughly correspond to what is expected in a survey like BOSS [48]. The thick red dashed line shows the best fit that is obtained if we analyse this data with the P-model (i.e., a “wrong” bias model), marginalising over $0.9 < b_1 < 3$ and $10 < a < 60$ with flat priors. The minimum value of the χ^2 statistic (with $\nu = 100 - 3$ degrees of freedom) is indicated in the inset and suggests that this best fitting model cannot be rejected on statistical grounds. *Lower panel:* likelihood constraints on Ω_{m0} . The vertical grey dotted line indicates the input value of the mass density parameter Ω_{m0} . As in the upper panel, the thick red dashed line shows the result obtained from the power spectrum analysis by using the “wrong” P-model, which leads to a significant overestimation bias. The thin red dot-dot-dashed line shows the 1D likelihood profile obtained from the power spectrum analysis after marginalising over the biasing parameters of the “true” Q-model itself, which gives an unbiased result. These results are compared with those obtained by adopting the clustering ratio (with $x = 16h^{-1}\text{Mpc}$ and $n = 2$) as observable in the likelihood analysis, without implementing any marginalisation scheme. The corresponding likelihood profile is shown by the thick blue long dashed line. In addition, we also display with the blue thin dot-dashed line the likelihood profile obtained from the η -test when the data are generated with the P-model.

power spectrum in an ideal cubic galaxy survey whose side is $\sim 900h^{-1}\text{Mpc}$ (which roughly corresponds to the volume surveyed by BOSS). We assume Planck values for the relevant $P(k)$ parameters, in particular $\Omega_{m0} = 0.3175$. The galaxy power spectrum is then simulated by biasing the matter power spectrum with the Q-model. We then try to retrieve the input value of the matter density parameter by means of a Fisher analysis that uses as observable the shape of the power spectrum and which is run by marginalising over either the nuisance parameters

b_1 , Q of the Q-model (i.e. we analyse the data with the “true” biasing scheme) or the parameters b_1 , a of the P-model (i.e. we analyse the data with a “wrong” biasing scheme). In the bottom panel of FIG. 6, we show that constraints on Ω_{m0} obtained after marginalising over the correct biasing model are both accurate, the true value of Ω_{m0} is within the 1σ interval, and precise, although the relative imprecision of the measurement ($\sim 2.5\%$) is one order of magnitude larger than the imprecision ($\sim 0.2\%$) that could be attained if the values of the biasing parameters were perfectly known. On the other hand, if the power spectrum analysis is carried out by marginalising over the parameters of the “wrong” biasing model, the inferred value of Ω_m is systematically larger, and its 1σ error bar does not bracket anymore the true value.

For comparison, we also show in the lower panel of FIG. 6 the likelihood profiles obtained from the η -test, without any marginalisation, when the galaxy power spectrum is computed with either the Q-model or the P-model. As expected, the η -test shows a small sensitivity to the scale-dependence of the bias, as seen from the fact that the best-fit Ω_{m0} is not exactly the same if we use the Q-model or the P-model. However, in agreement with FIG. 6, in both cases the true value of Ω_{m0} is within the 1σ error bar of the likelihood. This again highlights the virtues of a probe that, being by construction less sensitive to scale-dependent bias, also minimises possible systematics induced by an improper marginalisation procedure.

In summary, we have shown that the clustering ratio can be used at the two percent level even though different biasing models with different ranges of parameters have been implemented. Moreover, the clustering ratio does not require to marginalise over poorly known biasing functions and parameters in modified gravity. Indeed, the required two percent accuracy can be attained without any marginalisation.

D. Nonlinear matter power spectrum

We have seen in the previous section that the galaxy clustering ratio can be estimated from the matter real-space clustering ratio. This greatly simplifies the analysis, but we still need to obtain sufficiently accurate predictions for the matter power spectrum itself. Indeed, the space volume occupied by the $s1$ and $s2$ samples forces us to evaluate the clustering ratio on scales x that are not large enough for linear perturbation theory to be consistently applied. On these quasi-linear scales, where high-order, model-dependent corrections to the power spectrum of matter cannot be in principle neglected, the density fluctuations are no longer separable functions of cosmic time t and scale k . Therefore, the η -statistics acquires a characteristic dependence on the redshift (see FIG. 2). In FIG. 7, we show the impact of including non-linear contributions to the power spectrum $P(k)$ when calculating the amplitude of the cluster-

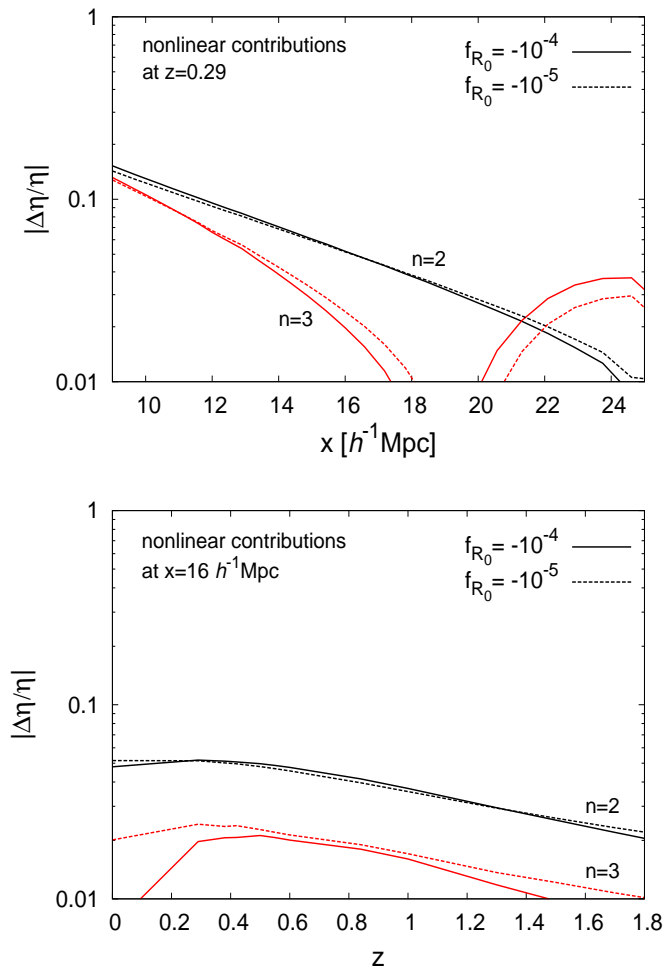


FIG. 7: Impact of non-linear contributions the power spectrum of matter on the amplitude of the clustering ratio, as a function of scale (*upper panel*) and redshift (*lower panel*). We show the relative deviation between η predictions obtained using the linear theory and the non-linear model described in [16].

ing ratio η_g^s . Specifically, we show the relative difference between the η amplitudes calculated by inserting into Eq.(5) either the linear matter power spectrum $P_L(k)$ or the non-linear model of [16] (a real-space matter power spectrum that is exact up to order P_L^2 in perturbation theory). At the characteristic scale $x = 16h^{-1}\text{Mpc}$, non-linear contributions to η modify linear expectations by only a few percents ($\simeq 6\%$ at $z = 0.29$ for $n = 2$, and much less for the larger correlation scale $n = 3$). Given that we aim at 2% accuracy, and since this inaccuracy is larger than the relative error with which the η statistics can be measured from current data ($\sim 3\%$), in what follows we will incorporate in our analysis these non-linear corrections to the power spectrum of matter. To this purpose, we use the analytical model described in [16, 61], which is exact up to one-loop order of perturbation the-

ory, and matches ΛCDM numerical simulations up to 2% at $r \geq 16h^{-1}\text{Mpc}$ for $\xi(r)$. In particular, as shown in [62], uncertainties due to non-perturbative small-scale effects, such as a change of up to 10% of the halo mass function or of the mass-concentration relation (or using different published fits) for the underlying halo model, only change $\xi(r)$ at $r \geq 16h^{-1}\text{Mpc}$ by less than 1%. Uncertainties in modeling the non-linear power spectrum of matter are thus expected to affect in a negligible way the clustering ratio statistics, at least on scales $x \geq 16h^{-1}\text{Mpc}$.

E. Baryonic effects.

On small cosmic scales, the matter density power spectrum is also sensitive to the physics of baryons and to galaxy formation processes, such as AGN feedback. However, from FIG. 5 of [63], numerical simulations suggest that these effects are small on large scales, $k < 1h\text{Mpc}^{-1}$ at $z = 0$, and only reach the level of the modification associated with an $F(R)$ model with $f_{R_0} = -10^{-5}$ at $k \gtrsim 7h\text{Mpc}^{-1}$. In configuration space, this leads to a damping of the density fluctuations on scales smaller than $6h^{-1}\text{Mpc}$. Therefore, by considering larger scales, above $16h^{-1}\text{Mpc}$ at $z \geq 0.29$, and restricting our analysis to $|f_{R_0}| \geq 10^{-5}$, we can safely neglect these effects. Interestingly, the η statistics is expected to be less sensitive to these local effects than the power spectrum $P(k)$. Indeed, the clustering ratio $\eta = \xi_x(r)/\sigma_x^2$, being a statistics defined in configuration space and smoothed over scale x , should be insensitive to redistributions of matter on smaller scales (whereas local motions typically lead to power law tails $\propto k^4$ for power spectra [64]).

F. Robustness of the η probe.

In conclusion, within the regime of quasi-linear filtering scales ($x = 16h^{-1}\text{Mpc}$) and moderate redshifts ($z < 0.67$) under investigation, the η statistics allows us to tell apart standard and non-standard models of gravity at the two percent level even without the need of correcting predictions with models for non-linear bias, non-linear galaxy motions, or linear bulk flows. However, the predicted amplitude of η is still sensitive, in the regimes under investigations, to the modelling of the non-linear power spectrum. Interestingly, however, FIG. 7 shows that the Euclid space mission will soon probe volumes of space large enough to make the estimation of η independent also from high order corrections of the matter power-spectrum. Indeed, once η is estimated for $n = 2$ on scales $x > 25h^{-1}\text{Mpc}$, these model-dependent corrections can be neglected to better than 1% accuracy.

One last point deserves mention. While for $f_{R_0} = -10^{-4} / -10^{-5}$ the relative deviation between $F(R)$ and ΛCDM predictions for the amplitude of η is larger than the precision with which the clustering ratio is currently measured (3%), this deviation becomes smaller

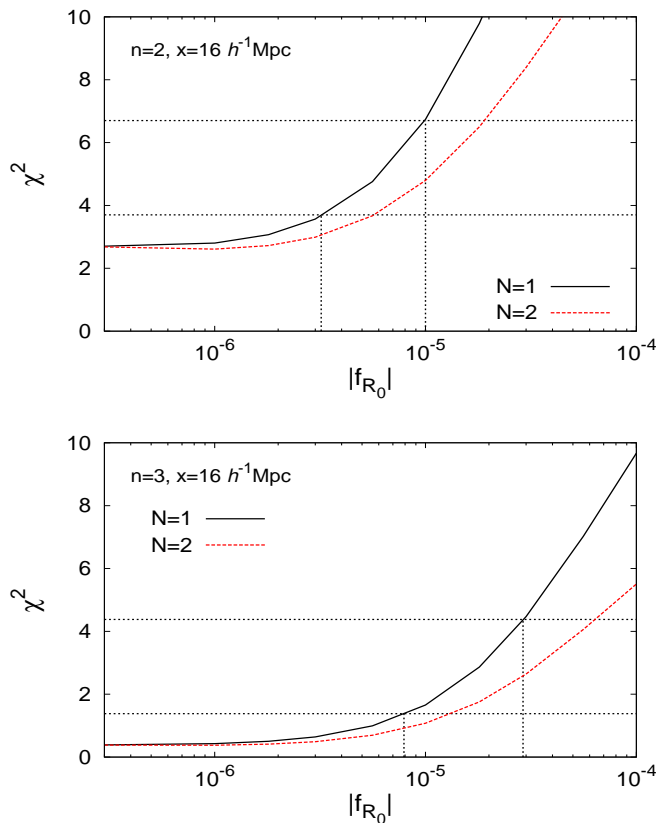


FIG. 8: χ^2 profile from the least square analysis of the clustering ratio data $\eta(n, x)$ measured from the SDSS samples $s1$ and $s2$ for $x = 16h^{-1}\text{Mpc}$ and in three different redshift bins at $z = 0.29, 0.42$, and 0.60 . We show results for the correlation indices $n = 2$ (upper panel) and $n = 3$ (lower panel). We consider $F(R)$ models with $N = 1$ (upper solid lines) and $N = 2$ (lower dashed lines). The horizontal dotted lines are the 68% and 95% confidence contours.

than $\sim 0.5\%$ for $|f_{R0}| < 10^{-6}$. Therefore, it is unlikely that constraints on $F(R)$ models with $|f_{R0}| < 10^{-6}$ be free of systematics unless the neglected effects or the residual systematics affect in the same way both the $F(R)$ and ΛCDM models.

IV. CONSTRAINTS ON $F(R)$ MODELS

We quantify the confidence level with which current data reject an $F(R)$ gravitational scenario by means of the standard χ^2 statistic. We do this by exploring two complementary scenarios. We first consider $F(R)$ models with exponents $N = 1$ or $N = 2$ and we assume that the background field value $|f_{R0}|$ is the only free fitting parameter. Therefore, in what we call hereafter *scenario 1*, we assume that the background expansion is exactly described by the reference ΛCDM model. By this choice we want to mimic the situation in which background data

have infinite precision and the discriminatory power on modified gravity parameter is provided only by perturbed sector data. This scenario also allows us to highlight, neatly, the specific virtues of the clustering ratio as a diagnostic of gravity. In *scenario 2* we take into account the uncertainty with which the background expansion history is presently known by allowing for an additional fitting parameter, the matter density parameter Ω_{m0} , which is not known to better than 6% (68% *c.l.* from Planck data). We still assume, however, that the expansion of the background is fairly described in terms of a flat ΛCDM model and that the remaining parameters to which η is sensitive, n_s , $\Omega_b h^2$, and H_0 , are fixed to their Planck value [their uncertainty (0.7%, 1.2%, 1.8% respectively) being negligible with respect to that of the matter density parameter]. An additional parametric dependence, specifically on the *rms* of matter fluctuations σ_8 , naturally arises as a consequence of estimating η on quasi-linear scales, i.e. on scales where this parameter controls the shape of the non-linear power spectrum of matter. On the scales explored in this paper, the functional dependence of η on σ_8 is however extremely weak. Indeed, although the relative uncertainty $\Delta\sigma_8/\sigma_8$ is rather large ($\sim 3\%$) if compared to the precision achieved by Planck on other parameters, varying σ_8 within the Planck 99.7% confidence interval only results in η changing by 0.2% at most (a figure that should be compared, for example, with the relative change with respect to the best fitting value $\delta\eta/\eta \sim -14\%(+18\%)$ when Ω_m is estimated at the upper(/lower) extrema of the Planck 99.7% confidence interval).

Because the signals at different scales x are correlated, we only analyse, in both scenarios, the galaxy field filtered on the scale $x = 16h^{-1}\text{Mpc}$, a trade-off between the precision of measurements (worsening as x increases) and of theory, i.e. of Eq.(5) (worsening as x decreases). We make separate analyses for the correlation indices $n = 2$ and 3 , hereafter called respectively *reference* analysis and *control* analysis. Note that the covariance matrix is diagonal, since the η measurements in the three different redshift bins can be considered as independent estimates.

The resulting 1D Log-likelihood profiles obtained from the analysis of the clustering ratio data in *scenario 1* are shown in FIG. 8. The most immediate conclusion drawn is that the reference ΛCDM model (the limiting case in which $|f_{R0}|$ goes to zero) is an excellent fit to the data. The null hypothesis that the reference ΛCDM does not provide a satisfactory description of clustering data is ruled out with a significance level of 25% (for $n = 2$) and 82% (for $n = 3$) computed as the probability of having a χ^2 statistic more extreme than 2.77 and 0.39 respectively. This result is at odds with results based on the analysis of the growth rate data which seems to favor models predicting slightly less growth of structures than the *reference* ΛCDM model [23, 27].

FIG. 8 also shows that the smaller the correlation index n the more discriminatory the η statistic in rejecting $F(R)$ scenarios is, essentially because of the smaller

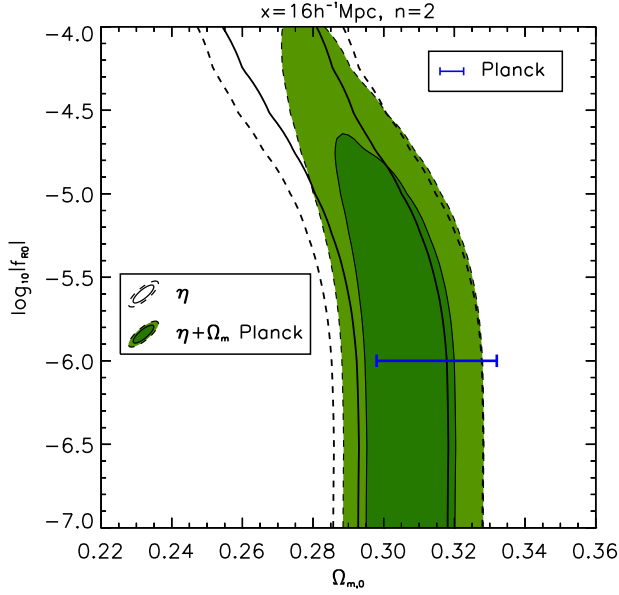


FIG. 9: Two-dimensional likelihood contours on Ω_{m0} and f_{R0} from the least square analysis of the clustering ratio $\eta(n, x)$ of the SDSS samples $s1$ and $s2$. The clustering ratio is estimated for $x = 16h^{-1}\text{Mpc}$ and $n = 2$ in three different redshift bins ($z = 0.29, 0.42$, and 0.60). Contours corresponds to 68 and 95 per cent *c.l.* for a multivariate Gaussian distribution with 2 degrees of freedom. Black contours show the results obtained by fixing the baryon density $\Omega_b h^2 = 0.0221$, the Hubble constant $H_0 = 67.4 \text{ km s}^{-1} \text{ Mpc}^{-1}$ and the scalar spectral index $n_s = 0.96$ but letting Ω_{m0} as a free parameter. Green shaded areas show the results after implementing the Planck Gaussian prior $\Omega_{m0} = 0.315 \pm 0.017$. We consider $F(R)$ models with $N = 1$.

error bars (see FIG. 2). Interestingly, while the reference analysis ($n = 2$) provides stronger constraints, $|f_{R0}| \lesssim 3.2 \times 10^{-6} / (5.6 \times 10^{-6})$ to the 68% precision level in $F(R)$ models with the exponent $N = 1(2)$ (and $|f_{R0}| \lesssim 9.9 \times 10^{-6} / (1.9 \times 10^{-5})$ at the 95% level), the control analysis ($n = 3$), being run on different correlation scales, allows us to check the unbiasedness of our conclusions. We also remark that $F(R)$ models with higher exponent N are progressively less constrained since, when compared to the $N=1$ models, they display a faster convergence to the ΛCDM model at high redshift.

Joint 2D likelihood contours on Ω_{m0} and f_{R0} obtained in *scenario 2* are displayed in FIG. 9. The degeneracy between Ω_{m0} and f_{R0} is essentially due to the fact that the shape of the power spectrum is regulated in a similar way by these two quantities (power is enhanced on small scales as the matter density increases or gravity becomes stronger on mildly non-linear scales). Incidentally, we note that this degeneracy might be somewhat alleviated if clustering ratio measurements were available at redshifts higher than those analysed here. Indeed the power spectrum becomes progressively insensitive to modified-gravity effects at earlier epochs.

Despite this degeneracy, it is interesting to note that

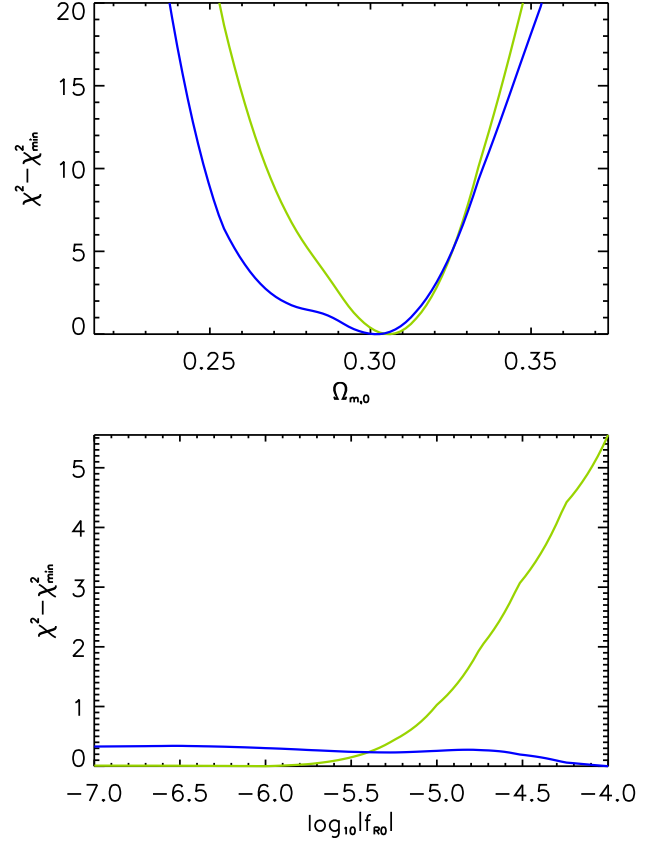


FIG. 10: Marginalised 1D likelihood constraints on Ω_{m0} (upper panel) and f_{R0} (lower panel). The green/blue curves show the results obtained with/without the Gaussian Planck prior on Ω_{m0} .

even allowing for modification of gravity, there is a neat upper bound to the value of the matter density parameter that is compatible with clustering ratio measurements, specifically $\Omega_{m0} < 0.328$ at 95% confidence level. This is most clearly seen in FIG. 10 where the marginalised 1D likelihood of the matter density parameter is shown. The Planck prior on the matter density parameter does not ameliorate the already strong constraints set by the η test for $\Omega_{m0} > \Omega_{m0}^{\text{best fit}}$. Indeed the situation is the opposite, that is, the η constraint on Ω_{m0} improves by nearly a factor of two the precision on the matter density parameter obtained by Planck (nearly 6% precision at 95% *c.l.*). As a consequence, all ΛCDM and $F(R)$ models analysed in this paper with a parameter $\Omega_{m0} > 0.328$ are rejected by the η test alone. In other words, the upper bound on the matter density parameter obtained within a ΛCDM model from these observations cannot be relaxed by invoking any modification of gravity of the form given in Eq. (6).

Notwithstanding, by imposing a lower bound to the possible variation of Ω_{m0} , that is $\Omega_{m0} > 0.298$ at 68%*c.l.*, the Planck prior allows us to exclude $F(R)$ models with $|f_{R0}| > 10^{-4}$ (see FIG. 9). The resulting 1D constraints

on f_{R_0} obtained by marginalising over the matter density parameter are shown in the lower panel of FIG. 10. This gives $|f_{R_0}| < 4.6 \times 10^{-5}$ at 95% *c.l.*.

These results should be compared to the bounds obtained from other observables. The joint analysis of several large-scale tracers (baryon acoustic oscillations (BAO), power spectrum, lensing, galaxy flows) combined with WMAP data gives $B_0 < 1.1 \times 10^{-3}$ at 95% *c.l.* [53], where B_0 is defined as $B_0 = f_{RR}/(1 + f_R)R'H/H'$. This corresponds to $|f_{R_0}| < 8.4 \times 10^{-4}$, for $N = 1$ [the parameterization (6) gives $B_0 = -2f_{R_0}(N + 1)/(1 + 3\Omega_\Lambda)$]. On cosmological scales, the best bound is $B_0 < 8.5 \times 10^{-5}$, from the combined likelihood of the temperature power-spectrum of Planck, of the galaxy power spectrum from the wiggleZ data on scales larger than $30h^{-1}\text{Mpc}$, and, at lower redshift, of the baryon acoustic oscillation (BAO) measurements from the 6dF Galaxy Survey, SDSS DR7 and BOSS DR9 [54]. This corresponds to $|f_{R_0}| < 6.5 \times 10^{-5}$, for $N = 1$. The clustering ratio of SDSS DR10 data, being able to delve into the quasi-linear part of the power spectrum where deviations from GR are larger than on linear scales, allows one to get comparable constraints using data from a single sample and a prior on Ω_{m0} (from Planck). Stronger constraints are expected when the η statistics is combined with other gravity probes [55].

On smaller scales of a few kpc's, strong gravitational lensing effects of galaxies place a bound $|f_{R_0}| \lesssim 2.5 \times 10^{-6}$ [57], which is stronger than the one from the linear power spectrum and of the same order as the one obtained using the clustering ratio. The absence of disruption of the dynamics of satellite galaxies of the Milky Way implies that the latter must be screened, implying a loose bound of $|f_{R_0}| \lesssim 7 \times 10^{-7}$ [56].

Effects on distance indicators in dwarf galaxies [7], and the comparison between the gas and stellar dynamics in these galaxies [8] imply that $|f_{R_0}| \lesssim 5 \times 10^{-7}$. Finally, the most severe constraint in the Solar System comes from the test of the strong equivalence principle by the Lunar Ranging experiment [6] at the 10^{-13} level, which results in a competitive bound $|f_{R_0}| \lesssim 10^{-6}$ for $N = 1$ and irrelevant ones for greater values of N .

All in all, we find that the clustering ratio provides a method to test the properties of modified gravity almost as sharp as Solar System experiments such as Lunar Ranging or strong lensing observations, and better than current observations of the growth of cosmological structures on linear scales. Only dwarf galaxies where the chameleon effects are enhanced between screened and unscreened objects are more discriminatory.

Looking into the future, we have used the Horizon mock surveys [58] to extrapolate some forecasts for the errors on η achievable by Euclid, a future redshift survey with characteristics similar to SDSS, but covering larger and deeper space volumes. Computations in *scenario 1*, *i.e.* by assuming the precise knowledge of the background cosmology, show that such a mission will be able to push the statistical error on measurements of η

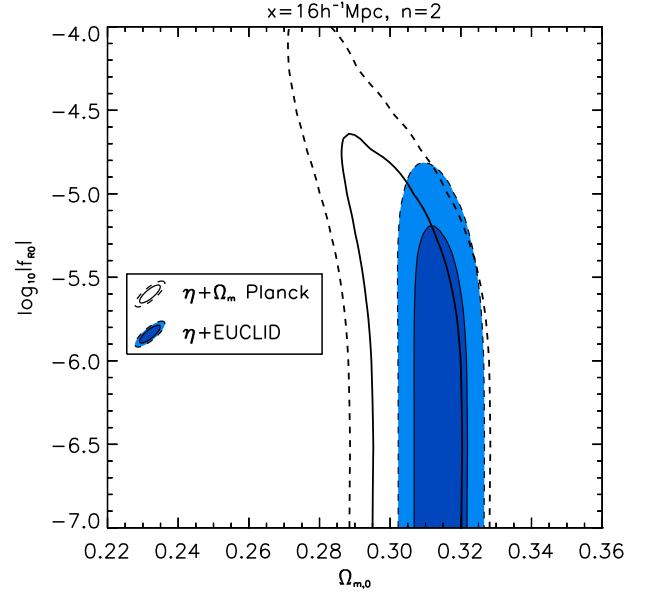


FIG. 11: Two-dimensional likelihood contours on Ω_{m0} and f_{R_0} from the least square analysis of the clustering ratio $\eta(n, x)$ of the SDSS samples *s1* and *s2*. The clustering ratio is estimated for $x = 16h^{-1}\text{Mpc}$ and $n = 2$ in three different redshift bins ($z = 0.29, 0.42$, and 0.60). Contours corresponds to 68 and 95 per cent *c.l.* for a multivariate Gaussian distribution with 2 degrees of freedom. Black contours show the results obtained by fixing the baryon density $\Omega_b h^2 = 0.0221$, the Hubble constant $H_0 = 67.4 \text{ km s}^{-1} \text{ Mpc}^{-1}$ and the scalar spectral index $n_s = 0.96$ but letting Ω_{m0} as a free parameter. Blue shaded areas show the results after combining with the expected constraints from Euclid. We consider $F(R)$ models with $N = 1$.

at $z \sim 1/(1.5)$ below 0.9%/(1.1%) (we consider $n = 2$ and $x = 16h^{-1}\text{Mpc}$). We find that, although the clustering ratio in $F(R)$ scenarios significantly differs from that expected in the ΛCDM model only at late epochs, when cosmic acceleration kicks in, high redshift Euclid measurements are expected to lower the 95% bound on f_{R_0} by roughly a factor of 4. Therefore, even in the near future, cosmological constraints on $F(R)$ gravity are not expected to improve on astrophysical bounds. This result is specific to models with the chameleon property. The analysis of alternative screening mechanisms like K-mouflage [60], where large objects such as galaxy clusters are not screened, will certainly make Euclid-like data more discriminatory. A similar improvement is seen when allowing for uncertainties in the knowledge of the matter density parameter (*scenario 2*). Indeed FIG. 11 shows that the combination of high (EUCLID) and low (SDSS) redshift estimates of the galaxy clustering ratio will allow to break the degeneracy between f_{R_0} and Ω_{m0} . As a result, the 95% upper bound on f_{R_0} is expected to decrease down to $\sim 10^{-5}$, nearly a factor 5 improvement on current constraints.

V. CONCLUSION

We have extended the clustering ratio method to the study of modified gravity models in their cosmological regime and in the quasi-linear regime of structure formation. We have shown that the accuracy of the comparison between the theoretical calculation of the clustering ratio and data reaches 2%. Using the $F(R)$ models in the large curvature regime as a template for modified gravity, we find that this is enough to obtain competitive bounds on parameters such as f_{R_0} when the matter fraction is fixed or allowed to vary within a prior given by Planck. In the first case, we find that the bound on $|f_{R_0}| \lesssim 3 \times 10^{-6}$ (at the 68% confidence level) is of the same order as the one from the Solar System. This also gives a 10^{-5} bound at the 95% confidence level. In the second case, the 95% *c.l.* bound becomes $|f_{R_0}| \lesssim 4.6 \times 10^{-5}$. This is slightly better than the cosmological limit obtained in the linear regime of perturbation theory.

More precisely, having assumed that Planck measurements provide an accurate mapping of redshifts into distances, i.e a precise description of the smooth expansion rate history of the Universe, we have shown that the reference Λ CDM model describes the linear clustering properties of SDSS galaxies in the redshift range $0.15 < z < 0.67$, that is Einstein's General Relativity satisfactorily describes also the perturbed dynamics of the late Universe. In particular, by fixing the relevant cos-

mological parameters to the Planck central value, $F(R)$ models having the same expansion rate as the reference Λ CDM model are excluded at 95% by the η -test of gravity if $|f_{R_0}| > 10^{-5}$ (if Ω_{m0} is fixed) and $|f_{R_0}| > 4.6 \times 10^{-5}$ (if we have a Planck Gaussian prior on Ω_{m0}). Based on this encouraging result, an extensive likelihood analysis is being conducted with the aim of using the η statistic to assess the viability of a more general class of modified gravity models, such as dilaton and symmetron models [15, 16], which can exhibit greater deviations from Λ CDM, or K -mouflage models [59, 60], where both the background and the perturbations deviate from Λ CDM.

Acknowledgments

We acknowledge useful discussions with L. Perenon and F. Piazza. CM is grateful for support from specific project funding of the Institut Universitaire de France and of the Labex OCEVU. JB acknowledges support of the European Research Council through the Darklight ERC Advanced Research Grant (#291521). This work is supported in part by the French Agence Nationale de la Recherche under Grant ANR-12-BS05-0002. P.B. acknowledges partial support from the European Union FP7 ITN INVISIBLES (Marie Curie Actions, PITN-GA-2011- 289442) and from the Agence Nationale de la Recherche under contract ANR 2010 BLANC 0413 01.

-
- [1] S. Perlmutter et al. (Supernova Cosmology Project), *Astrophys. J.* **517**, 565 (1999)
 - [2] A. G. Riess et al. (Supernova Search Team), *Astron.J.* **116**, 1009 (1998), [astro-ph/9805201](#).
 - [3] J. P. Ostriker and P. Steinhardt, *New Light on Dark Matter*, *Science*, **300**, 1909 (2003)
 - [4] C. S. Frenk and S.D. M. White, *Ann. Phys.*, **524**, 507 (2012)
 - [5] T. Clifton, P. G. Ferreira, A. Padilla, and C. Skordis, *Physics Reports*, **513**, 1 (2012)
 - [6] J. G. Williams, S. G. Turyshev and D. Boggs, *Class. Quant. Grav.* **29** (2012) 184004.
 - [7] B. Jain, V. Vikram and J. Sakstein, *Astrophys. J.* **779** (2013) 39.
 - [8] V. Vikram, A. Cabre, B. Jain and J. T. VanderPlas, *JCAP* **1308** (2013) 020.
 - [9] A. Vainshtein, *Phys.Lett.* **B39**, 393 (1972).
 - [10] T. Damour and A. M. Polyakov, *Nucl. Phys. B* **423**, 532 (1994).
 - [11] J. Khoury and A. Weltman, *Phys.Rev.Lett.* **93**, 171104 (2004).
 - [12] J. Khoury and A. Weltman, *Phys. Rev. D* **69**, 044026 (2004).
 - [13] P. Brax, C. van de Bruck, A.-C. Davis, J. Khoury, and A. Weltman, *Phys. Rev. D* **70**, 123518 (2004).
 - [14] R. Bean, D. Bernat, L. Pogosian, A. Silvestri, M. Trodden, *Phys. Rev. D*, **75**, 4020 (2007).
 - [15] Ph. Brax, P. Valageas, *Phys. Rev. D*, **86**, 063512 (2012).
 - [16] Ph. Brax, P. Valageas, *Phys. Rev. D*, **88**, 023527 (2013).
 - [17] B. Hu, M. Raveri, N. Frusciante, and A. Silvestri, [arXiv:1312.5742](#)
 - [18] A. Lue, R. Scoccimarro and G. D. Starkman, *Phys. Rev. D* **69**, 124015 (2004)
 - [19] F. Piazza, H. Steigerwald and C. Marinoni, *JCAP*, **05**, 043 (2014) [arXiv:1312.6111](#)
 - [20] S. Tsujikawa and T. Tatekawa, *Phys. Lett. B*, **665**, 325 (2008).
 - [21] F. Schmidt, *Phys. Rev. D* **78**, 3002 (2008)
 - [22] L. Guzzo, M. Pierleoni, B. Meneux, et al., *Nature*, **451**, 541 (2008).
 - [23] L. Samushia, B. A. Reid, M. White et al., [arXiv:1312.4899](#).
 - [24] L. Pogosian, A. Silvestri, *Phys. Rev. D*, **77**, 023503 (2008).
 - [25] H. Oyaizu, M. Lima, W. Hu, *Phys. Rev. D*, **78**, 123524 (2008).
 - [26] M. Motta, I. Sawicki, I.D. Saltas, et al., *Phys. Rev. D*, **88**, 124035 (2013).
 - [27] H. Steigerwald, J. Bel and C. Marinoni, *JCAP* **05** 042, (2014) [arXiv:1403.0898](#)
 - [28] V.F. Cardone, S. Camera, A. Diaferio, *JCAP*, **02**, 030 (2012).
 - [29] A. Taruya, K. Koyama, T. Hiramatsu, and A. Oka *Phys. Rev. D* **89**, 043509.
 - [30] A. Nusser, E. Branchini and M. Davis, *ApJl*, **744**, 7 (2012).

- [31] J. Bel and C. Marinoni, *A&A*, 563, A36 (2014), arXiv:1310.3196
- [32] J. Bel, C. Marinoni, B. Granett et al. (The VIPERS Collaboration) *A&A*, 563, A37 (2014), arXiv:1310.3380
- [33] J. Bel and C. Marinoni, 2012, *MNRAS*, 424, 971
- [34] M. Biagetti, V. Desjacques, A. Kehagias and A. Riotto, 2014, *PhRvD*, 90, 5022
- [35] J. N. Fry and E. Gaztañaga, 1993, *ApJ*, 413, 447
- [36] C. Marinoni et al. 2005, *A&A* 442, 801, arXiv:0506561
- [37] C. di Porto et al. 2014, arXiv:1406.6692
- [38] S. E. Nuza, A. G. Sánchez, F. Prada et al., 2013, *MNRAS*, 432, 743
- [39] N Kaiser, 1987, *MNRAS*, 227, 1
- [40] P. A. R. Ade et al., arXiv:1303.5076
- [41] E. Jennings, C. M. Baugh and S. Pascoli, 2010, *MNRAS*, 410, 2081
- [42] R. Scoccimarro, 2004, *PRD*, 70, 083007
- [43] R. Laureijs et al., arXiv:1110.3193 (2011).
- [44] S. M. Carroll, V. Duvvuri, M. Trodden and M. S. Turner, *Phys. Rev. D*, 70.043528 (2004).
- [45] T. P. Sotiriou and V. Faraoni *Rev. Mod. Phys.*, 82, 451 (2010).
- [46] W. Hu and I. Sawicki, *Phys. Rev. D*, 76, 064004 (2007).
- [47] K. N. Abazajian et al., *ApJS* **182**, 543 (2009).
- [48] C. P. Ahn et al., *ApJS*, **211**, 17 (2014).
- [49] C. McBride et al., *AAS*, 21342506 (2009)
- [50] S. Cole, W. Percival, J. Peacock et al. *MNRAS*, 362, 505 (2005)
- [51] J. G. Cresswell, W. J. Percival, *MNRAS*, 392, 682 (2008)
- [52] R.E. Smith, R. Scoccimarro, R. Sheth *Phys Rev D* 75 063512 (2007)
- [53] L. Lombriser, A. Slosar, U. Seljak, and W. Hu, *Phys. Rev. D* 85 (2012) 124038
- [54] J. Dossett, B. Hu and D. Parkinson, *JCAP* **1403** (2014) 046.
- [55] J. Bel et al., in preparation
- [56] L. Lombriser, *Annalen Phys.* **526** (2014) 259.
- [57] T. L. Smith, arXiv:0907.4829 [astro-ph.CO].
- [58] J. Kim, C. Park, J. R. Gott III, and J. Dubinski, 2009, *ApJ*, 701, 1547.
- [59] Ph. Brax, P. Valageas, *Phys. Rev. D*, 90, 023507 (2014).
- [60] Ph. Brax, P. Valageas, *Phys. Rev. D*, 90, 023508 (2014).
- [61] P. Valageas, T. Nishimichi, A. Taruya, *Phys. Rev. D*, 87, 083522 (2013).
- [62] P. Valageas, *Phys. Rev. D*, 88, 083524 (2013).
- [63] E. Puchwein, M. Baldi, V. Springel, *MNRAS*, 436, 348 (2013).
- [64] P.J.E. Peebles, *A&A*, 32, 391 (1974).
- [65] The deviation from Λ CDM is not ten times smaller for $f_{R0} = -10^{-5}$ than for $f_{R0} = -10^{-4}$ because the transition scale $2\pi/(am)$ of the kernel $\epsilon(k, z)$ of Eq.(7) becomes closer to the scales $x = 16h^{-1}\text{Mpc}$ and $r = nx$ that we probe. Thus, at $z = 0.29$ we have $am \simeq 0.038/(0.119)h\text{Mpc}^{-1}$ for $f_{R0} = -10^{-4}(-10^{-5})$, which gives $2\pi/(am) \simeq 166(/53)h^{-1}\text{Mpc}$.